CHAPTER 10

Kilohertz-Driven Bose–Einstein Condensates in Optical Lattices

Ennio Arimondo[a,b,c], **Donatella Ciampini**[a,b,c], **André Eckardt**[d], **Martin Holthaus**[e] and **Oliver Morsch**[a,b]

[a]*Dipartimento di Fisica "E. Fermi", Università di Pisa, Largo Pontecorvo 3, 56127 Pisa, Italy*
[b]*INO-CNR, Largo Pontecorvo 3, 56127 Pisa, Italy*
[c]*CNISM UdR Università di Pisa, Largo Pontecorvo 3, 56127 Pisa, Italy*
[d]*Max-Planck-Institut für Physik komplexer Systeme, Nöthnitzer Straße 38, D-01187 Dresden, Germany*
[e]*Institut für Physik, Carl von Ossietzky Universität, D-26111 Oldenburg, Germany*

Contents

Abstract

We analyze time-of-flight absorption images obtained with dilute Bose–Einstein condensates released from shaken optical lattices, both theoretically and experimentally. We argue

Advances in Atomic, Molecular, and Optical Physics, Volume 61, Copyright © 2012 Elsevier Inc.
ISSN 1049-250X, http://dx.doi.org/10.1016/B978-0-12-396482-3.00010-7.

that weakly interacting, ultracold quantum gases in kilohertz-driven optical potentials constitute equilibrium systems characterized by a steady-state distribution of Floquet-state occupation numbers. Our experimental results consistently indicate that a driven ultracold Bose gas tends to occupy a single Floquet state, just as it occupies a single energy eigenstate when there is no forcing. When the driving amplitude is sufficiently high, the Floquet state possessing the lowest mean energy does not necessarily coincide with the Floquet state connected to the ground state of the undriven system. We observe strongly driven Bose gases to condense into the former state under such conditions, thus providing nontrivial examples of dressed matter waves.

1. INTRODUCTION

There is a growing interest in ultracold atoms confined in time-periodically driven optical lattices. It was pointed out already in 1997 that a metal–insulator-like transition of ultracold atoms in quasiperiodic optical lattices could be induced by changing the amplitude of a time-periodic driving force (Drese & Holthaus, 1997). The field became truly active only 10 years later, however, following the unambiguous experimental observations by the Pisa group of dynamical tunneling suppression in Bose–Einstein condensates and driving-induced reversal of the sign of the tunneling matrix element (Lignier et al., 2007). Related single-particle experiments were performed with driven double-well potentials in Heidelberg (Kierig et al., 2008). Several groups then have monitored the dynamics under the combined action of both a homogeneous time-independent and a time-periodic driving force, either with non-condensed cold atoms (Alberti et al., 2009; Ivanov et al., 2008), or with Bose–Einstein condensates (Haller et al., 2010; Sias et al., 2008); such dynamics may be viewed as an analog of photon-assisted tunneling (Eckardt et al., 2005a). The Pisa group subsequently also reported the coherent control of the superfluid-to-Mott insulator transition in shaken three-dimensional optical lattices (Zenesini et al., 2009).

The recent detection of spontaneous breaking of time-reversal symmetry with fast-oscillating triangular optical lattices by Struck et al. (2011) constitutes a further milestone in this line of research. Moreover, photon-assisted tunneling in a strongly correlated Bose gas has very recently been investigated, possibly allowing for applications to topological physics and quantum computing (Ma et al., 2011). Also, active control of correlated tunneling in ac-driven optical superlattices has been observed, providing a novel approach to the realization of XXZ spin models (Chen et al., 2011).

On the theoretical side, several studies indicate promising future pathways: Eckardt and Holthaus (2008b) have suggested carrying out avoided-level-crossing spectroscopy for probing resonances which endanger the adiabatic control achievable through time-periodic forcing, while Eckardt et al. (2010) have worked out a proposal for simulating frustrated quantum antiferromagnetism with oscillating triangular lattices. Later Tokuno and Giamarchi (2011) have pointed out that a small periodic phase modulation of an optical lattice can give direct access to the system's conductivity. Furthermore, Tsuji et al. (2011) have argued that ac forcing may even change the interparticle interaction from repulsive to attractive, thereby enabling one to simulate an effectively attractive Hubbard model with a temperature below the superconducting transition temperature.

On a first superficial glance, ultracold atoms in shaken optical lattices, with shaking frequencies on the order of a few to tens of kilohertz, might appear as typical examples of nonequilibrium systems. But this naive view is not correct. Quantum systems governed by a time-periodic Hamiltonian possess a particular basis, consisting of Floquet states, with respect to which one finds occupation numbers which remain *constant* in time, with the periodic time-dependence already being incorporated into the basis states themselves. Thus, a weakly interacting quantum gas subjected to time-periodic forcing, and possibly exposed to some sort of noise, will be statistically characterized by a time-independent distribution of Floquet-state occupation numbers. What is that *equilibrium* distribution?

In the present tutorial article we develop this line of thought, and discuss experimental data, obtained with Bose–Einstein condensates in kilohertz-shaken optical lattices, which we interpret as evidence for Floquet-based dynamics. We proceed as follows: In Section 2 we review basic elements of the Floquet picture, and speculate about the existence of analogs of the Bose–Einstein and the Fermi–Dirac distribution function for isolated, time-periodically driven quantum gases. We then turn in Section 3 to the realization of periodically shaken optical lattices, and extending previous analyses (Madison et al., 1997; Peik et al., 1997) we pay particular attention to the distinction between the co-moving frame of reference, in which the trapped quantum gas experiences a spatially homogeneous inertial force, and the laboratory frame, in which the measurements are performed. In Section 4 we briefly introduce the driven Bose–Hubbard model (Eckardt et al., 2005b). In Section 5 we calculate momentum distributions expected in time-of-flight absorption imaging for matter waves occupying a single Floquet state. We consider two particular situations: An interacting gas periodically driven at high frequencies, and a noninteracting gas subjected to a force with arbitrary time-dependence. Here we also point out certain characteristic differences between time-of-flight absorption images obtained from shaken lattices utilizing the inertial force, and the corresponding images acquired when the lattice remains at rest, while the force

is exerted, e.g., through the harmonic modulation of a levitation gradient (Haller et al., 2010). In Section 6 we tie the various strands together and report our measurements, which suggest the existence of Floquet condensates occupying the "lowest" available Floquet state. While we consider only one comparatively simple experimental setting, it appears likely that our findings are of a more general nature. In the final Section 7 we briefly spell out our main conclusions.

2. THE QUEST FOR FLOQUET CONDENSATES

The notion of Bose–Einstein condensation of an almost ideal gas (Einstein, 1924, 1925; London, 1938) appears to be inextricably linked to the energy eigenstates of some single-particle Hamiltonian: When the temperature of a gas of weakly interacting Bose particles becomes lower than a certain critical temperature, the gas "condenses" into the single-particle ground state, meaning that this ground state becomes macroscopically occupied. It might seem that this concept cannot be applied to explicitly time-dependent systems, for which, in general, there are no stationary states. Yet, there is one notable exception: If a single-particle Hamiltonian $H^{(1)}(t)$ is periodic in time, so that $H^{(1)}(t) = H^{(1)}(t+T)$ for some period T, then Floquet's theorem (Floquet, 1883; Kuchment, 1993) suggests the existence of a set of distinguished solutions $|\psi_n(t)\rangle$, known as Floquet states, to the time-dependent Schrödinger equation $\mathrm{i}\hbar\partial_t|\psi(t)\rangle = H^{(1)}(t)|\psi(t)\rangle$; these Floquet states are in many ways analogous to the usual energy eigenstates of time-independent Hamiltonian operators (Breuer & Holthaus, 1991; Chu & Telnov, 2004; Ritus, 1967; Shirley, 1965; Sambe, 1973; Zel'dovich, 1967). They have the particular form

$$|\psi_n(t)\rangle = |u_n(t)\rangle \exp(-\mathrm{i}\varepsilon_n t/\hbar), \tag{1}$$

where the functions $|u_n(t)\rangle = |u_n(t+T)\rangle$ inherit the period T of the underlying Hamiltonian; the index n denotes a set of quantum numbers specifying the state. The quantities ε_n, which determine the phase factors accompanying the time-evolution of the Floquet states (1) in the same manner that the energy eigenvalues of time-independent systems determine the phase factors appearing in the evolution of the state vector, are dubbed quasienergies (Ritus, 1967; Zel'dovich, 1967).

There is a compelling reason for considering these Floquet states. Namely, at each instant t_0 the set of Floquet functions $\{|u_n(t_0)\rangle\}$ is complete in the physical Hilbert space on which $H^{(1)}(t)$ acts. Hence, *any* solution $|\psi(t)\rangle$ to the time-dependent Schrödinger equation admits an expansion of the form

$$|\psi(t)\rangle = \sum_n c_n |u_n(t)\rangle \exp(-\mathrm{i}\varepsilon_n t/\hbar) \tag{2}$$

with *time-independent* coefficients c_n. Therefore, under conditions of perfectly coherent evolution the occupation probabilities $|c_n|^2$ of the Floquet states remain constant, despite the periodic time-dependence of the Hamiltonian. These coefficients then keep a memory of how the system has been prepared, that is, how the time-periodic forcing has been turned on in the past, whereas the Floquet states and their quasienergies are independent of this history.

If, however, the evolution is not coherent, but the system is in contact with some sort of thermal environment or heat bath, what would be the equilibrium distribution of the Floquet-state occupation probabilities which establishes itself in the long run, irrespective of the particular initial condition? An important step towards a general answer to this question has been taken by Breuer et al. (2000), who have studied anharmonic oscillators subjected to strong time-periodic forcing while being weakly coupled to thermal degrees of freedom provided by a surrounding, and who have shown that the corresponding quasistationary density matrix actually is diagonal in the Floquet representation. This line of investigation has recently been taken up by Ketzmerick and Wustmann (2010), with a detailed view on the classical-quantum correspondence, after general aspects of such "periodic thermodynamics" had been discussed by Kohn (2001).

Turning now from the single-particle dynamics to that of an ideal gas of identical quantum particles subjected to some periodically time-dependent external influence, such as a dilute gas of Bose particles stored in a confining potential which is modulated periodically in time, an even more intriguing question poses itself: What are the statistics of the Floquet-state occupation numbers? In other words, what is the replacement for the familiar Bose–Einstein (or Fermi–Dirac, when dealing with fermions) distribution function in a periodically time-dependent setting?

In order to appreciate what lies behind this question, let us briefly retrace the steps which led Einstein (1925) to what is now known as Bose–Einstein statistics (Pathria, 1996): Consider an isolated ideal Bose gas consisting of $N \gg 1$ particles possessing a total energy E_{tot}, being kept in some large confinement. In view of the corresponding denseness of the single-particle spectrum we divide the energy axis into small intervals, the ith such interval containing g_i single-particle states with practically identical energy E_i. We then denote the number of particles occupying the g_i states in the ith interval as n_i, and ask for the most probable set $\{n_i^*\}$ of these cell occupation numbers. All admissible sets $\{n_i\}$ obviously have to comply with the two constraints

$$\sum_i n_i = N \tag{3}$$

and

$$\sum_i n_i E_i = E_{\text{tot}}; \tag{4}$$

the latter holding approximately, reflecting the above coarse-graining procedure, but to good accuracy. The number of microstates associated with a given set $\{n_i\}$ is

$$\Omega[\{n_i\}] = \prod_i \binom{n_i + g_i - 1}{n_i}, \tag{5}$$

because the binomial coefficients quantify the number of possibilities to distribute n_i indistinguishable particles over g_i states "with repetition," as is characteristic for bosons. Assuming that both $n_i \gg 1$ and $g_i \gg 1$, and employing Stirling's formula, one then obtains the entropy:

$$\ln \Omega[\{n_i\}] = \sum_i \left[n_i \ln\left(1 + \frac{g_i}{n_i}\right) + g_i \ln\left(\frac{n_i}{g_i} + 1\right)\right]. \tag{6}$$

The searched-for most probable occupation numbers $\{n_i^*\}$ maximize this expression, subject to the two constraints (3) and (4). Introducing a Lagrangian multiplier α to account for the conservation of the particle number, and a further multiplier β to account for the conservation of energy, we are thus led to the variational problem:

$$\delta\left(\ln \Omega[\{n_i\}] - \alpha \sum_i n_i - \beta \sum_i n_i E_i\right)_{n_i = n_i^*} = 0. \tag{7}$$

After brief calculation, this gives

$$\sum_i \left[\ln\left(1 + \frac{g_i}{n_i}\right) - \alpha - \beta E_i\right]_{n_i = n_i^*} \delta n_i = 0 \tag{8}$$

and thus results in the Bose–Einstein distribution

$$\frac{n_i^*}{g_i} = \frac{1}{\exp(\beta E_i + \alpha) - 1}, \tag{9}$$

quantifying the most probable occupation number of an individual single-particle state with energy E_i under microcanonical conditions. Finally, the multiplier β is identified with $1/(k_{\text{B}}T)$, with k_{B} denoting Boltzmann's constant and T being the temperature of the gas, while $\alpha = -\mu/(k_{\text{B}}T)$ is related to its chemical potential μ (Einstein, 1925; Pathria, 1996).

When trying to adapt this reasoning to time-periodically driven quantum gases, and to determine the corresponding Floquet-state occupation numbers, we can immediately carry over the first constraint (3): The sum

of all occupation numbers has to equal the total number of particles. This may seem trivial, but it is not, because we are making essential use of Floquet theory: It is only because the coefficients c_n in the expansion (2) are time-independent that we can assign occupation numbers to the Floquet states; only then can one ask for the associated distribution function.

It is, however, not obvious what becomes of the second constraint (4), because energy eigenvalues do not exist for a time-periodic system, and the quasienergies of the Floquet states cannot be considered as their proper substitutes in this context. To understand the quasienergy concept more deeply, we insert the Floquet states (1) into the time-dependent Schrödinger equation, and deduce

$$\left(H^{(1)}(t) - \mathrm{i}\hbar\frac{\partial}{\partial t}\right)|u_n(t)\rangle\rangle = \varepsilon_n|u_n(t)\rangle\rangle. \tag{10}$$

The conspicuous notation employed here, i.e., writing the Floquet functions $|u_n(t)\rangle\rangle$ with a double right angle instead of $|u_n(t)\rangle$ as in Equation (1), has a deep significance. Namely, Equation (10) has to be regarded as an *eigenvalue equation* for the quasienergies; within the Floquet framework, this eigenvalue equation takes over the role played for time-independent systems by the stationary Schrödinger equation. Unlike the latter, this quasienergy eigenvalue Equation (10) lives in an *extended Hilbert space* of T-periodic functions (Sambe, 1973). In contrast to the usual physical setting, in which "time" emerges as an evolution variable, in that extended space time plays the role of a *coordinate*, and therefore needs to be integrated over in the associated scalar product: Denoting the momentary scalar product of two T-periodic functions $|u_1(t)\rangle$ and $|u_2(t)\rangle$ in the physical space as $\langle u_1(t)|u_2(t)\rangle$, their scalar product in the extended space reads (Sambe, 1973)

$$\langle\langle u_1|u_2\rangle\rangle \equiv \frac{1}{T}\int_0^T \mathrm{d}t\,\langle u_1(t)|u_2(t)\rangle. \tag{11}$$

Thus, we write $|u_n(t)\rangle$ when considering a Floquet function in the physical Hilbert space, as in Equations (1) and (2), whereas $|u_n(t)\rangle\rangle$ refers to that same function when viewed as an element of the extended space, as in Equation (10).

This apparently formal observation has an important, physically meaningful consequence. Suppose that $|u_n(t)\rangle\rangle$ is a solution to the eigenvalue Equation (10) with quasienergy ε_n, define $\omega = 2\pi/T$, and let m be an arbitrary (positive, zero, or negative) integer. Then $|u_n(t)\exp(\mathrm{i}m\omega t)\rangle\rangle$ also is a T-periodic solution, with quasienergy $\varepsilon_n + m\hbar\omega$. For $m \neq 0$ these two Floquet functions obviously are orthogonal with respect to the scalar product (11), and represent *different* eigenfunctions in the extended space. On the other hand, when returning to the physical space and forming the actual

Floquet states (1), one has

$$|u_n(t)\exp(\mathrm{i}m\omega t)\rangle\exp\left(-\mathrm{i}(\varepsilon_n+m\hbar\omega)t/\hbar\right)=|u_n(t)\rangle\exp(-\mathrm{i}\varepsilon_n t/\hbar), \quad (12)$$

so that both solutions represent *the same* physical state. Hence, a Floquet state does not correspond to a single solution to Equation (10), but rather to a whole class of such solutions, labeled by the index n, while individual representatives of such a class are distinguished by the integer m. This subtlety already reflects itself in the expansion (2): Although *all* functions $\{|u_n(t)\exp(\mathrm{i}m\omega t)\rangle\rangle\}$, with n ranging over all state labels and m extending over all integers, are required for the completeness relation in the extended space, *only one* representative from each class is required in Equation (2), where no sum over the "photon index" m appears. By the same token, the quasienergy of a physical Floquet state is determined only up to an integer multiple of the "photon" energy $\hbar\omega$. In accordance with the analogous terminology used in solid-state physics, the quasienergy spectrum is said to consist of an infinite set of identical "Brillouin zones" of width $\hbar\omega$, covering the entire energy axis, each state placing one of its quasienergy representatives in each zone. This means, in particular, that there is no natural "quasienergy ordering": Without additional specification it is meaningless to ask whether one given Floquet state lies "below" another. And there is still a further complication of a more mathematical nature: Because one finds one quasienergy representative of each state in each Brillouin zone, the quasienergy spectrum is "dense," and it may be technically difficult to decide whether one has a dense pure point spectrum, so that the expansion (2) can be taken literally and the system is stable, possessing a quasiperiodic wave function, or whether there is an absolutely continuous spectrum, allowing for diffusive energy growth (Bunimovich et al., 1991; Howland, 1992a). We bypass this problem by restricting ourselves to stable systems with a pure point spectrum, such as the forced anharmonic oscillators with superquadratic potentials investigated by Howland (1992b).

These considerations clearly reveal that, although there are Floquet-state occupation numbers, the required analog of the energy constraint (4) for time-periodically forced microcanonical close-to-ideal Bose gases cannot involve quasienergies directly. However, each Floquet state possesses a mean energy (Fainshtein et al., 1978)

$$\overline{E}_n \equiv \frac{1}{T}\int_0^T \mathrm{d}t\,\langle u_n(t)|H^{(1)}(t)|u_n(t)\rangle = \langle\langle u_n|H^{(1)}|u_n\rangle\rangle, \quad (13)$$

which obviously is independent of the choice of the representative $|u_n\rangle\rangle$. If we now repeat the coarse-graining procedure employed in the formulation of the energy constraint (4), that is, if we divide the energy axis into small cells, the ith cell now containing g_i Floquet states having almost the same mean energy $\overline{E}_i$, and if $\{n_i\}$ denotes the corresponding sets of cell occupation

numbers, then it seems reasonable to demand

$$\sum_i n_i \overline{E}_i = \text{const.} \tag{14}$$

for an isolated system, thus obtaining a constraint which effectively may replace the previous Equation (4). Here we assume that each driven particle sees the other driven particles as its heat bath, and undergoes subsequent short relaxation events only on a time scale which is large compared to the period T. In general, the justification of this constraint may require the consideration of particular physical setups, and some more specifications may be needed. But if we tentatively accept this constraint (14) as it stands, it is immediately clear how to proceed: We assign the entropy (6) to a time-periodically forced isolated Bose gas with Floquet-state occupation numbers $\{n_i\}$, account for the particle number conservation (3) again by introducing a Lagrangian multiplier α, and incorporate the conservation of the mean energy (14) with the help of a further Lagrangian multiplier γ. Then the most probable set of Floquet-state occupation numbers $\{n_i^*\}$ is determined by the variational equation

$$\delta \left(\ln \Omega[\{n_i\}] - \alpha \sum_i n_i - \gamma \sum_i n_i \overline{E}_i \right)_{n_i = n_i^*} = 0. \tag{15}$$

Because this problem exactly parallels the problem (7) already considered by Einstein (1925), we can directly take over the solution: Under the above conditions, the most probable set of Floquet-state occupation numbers is

$$\frac{n_i^*}{g_i} = \frac{1}{\exp(\gamma \overline{E}_i + \alpha) - 1}, \tag{16}$$

suggesting that

$$f(\overline{E}_n; \alpha, \gamma) = \frac{1}{\exp(\gamma \overline{E}_n + \alpha) - 1} \tag{17}$$

is the expected occupation number of an individual Floquet state with mean energy $\overline{E}_n$. Of course, this reasoning can easily be adapted to fermions, leading to the familiar "plus" sign in the denominator (Pathria, 1996).

These deliberations may have some profound physical implications. To begin with, a time-periodically forced, stable Bose gas manifestly does *not* constitute a nonequilibrium system, as one might naively assume, but rather an equilibrium one, with equilibrium parameters α and γ. Most noteworthy, these parameters depend on the form of the periodic time dependence, as do the Floquet states, and hence their mean energies (13), which enter into the modified constraint (14). Therefore, when writing

$$\gamma = \frac{1}{k_B \Theta} \tag{18}$$

in analogy to the familiar relation $\beta = 1/(k_B T)$, the parameter Θ introduced here is a temperature-like quantity which can be varied by changing, e.g., the strength of an external time-periodic force; in general, Θ will differ from the usual temperature T the gas would have if there were no such forcing. Likewise, when setting

$$\alpha = -\frac{\nu}{k_B \Theta}, \tag{19}$$

ν is the corresponding, forcing-dependent chemical potential.

It follows that there are *Floquet condensates*: If the Θ-temperature is sufficiently low, a time-periodically forced close-to-ideal Bose gas condenses into the single-particle Floquet state possessing the lowest mean energy. This deduction immediately suggests a further possibility: Suppose that the Hamiltonian under consideration has the natural form $H^{(1)}(t) = H_0 + H_1(t)$, where $H_1(t)$ represents a time-periodic force acting on the unperturbed system H_0 with adjustable strength. In the regime of perturbatively weak forcing the mean-energy ordering of the Floquet states of $H^{(1)}(t)$ is likely to be the same as the energy ordering of the eigenstates of H_0 from which they have developed, but in the nonperturbative regime this is no longer guaranteed; here the Floquet state possessing the lowest mean energy is not necessarily connected to the H_0-ground state. Under such conditions the Floquet state into which an ultracold, time-periodically forced Bose gas condenses is determined by the strength of the forcing, and may change when the latter is varied.

We close this section by emphasizing that the above reasoning hinges on two key issues: The assignment of occupation numbers to the Floquet states, which is borne out by theory, and the adoption of the mean-energy constraint (14) as a building principle for a microcanonical Floquet ensemble, which may require further thoughts. Important pieces of evidence supporting our theoretical deductions are provided by the experimental observations reported in Section 6 below. In order to facilitate the interpretation of our measurements, we first lay out some important ingredients in Sections 3–5.

3. THE EXPERIMENTAL SETUP: SHAKEN OPTICAL LATTICES

A one-dimensional (1D) optical lattice potential, which we write in the form:

$$V(x) = \frac{V_0}{2} \cos(2k_L x), \tag{20}$$

is generated by two linearly polarized counterpropagating beams of laser radiation with wave number k_L, its depth V_0 being proportional to the laser intensity (Morsch & Oberthaler, 2006). Here the lattice coordinate x refers to the laboratory frame of reference. Considering an atom of mass

M moving in this potential, the lattice depth V_0 is measured in units of its single-photon recoil energy E_r,

$$E_\mathrm{r} = \frac{\hbar^2 k_\mathrm{L}^2}{2M}; \tag{21}$$

typical optical lattices are up to tens of recoil energies deep. For example, when working with ^{87}Rb in an optical lattice made up from laser light with wavelength $\lambda = 2\pi/k_\mathrm{L} = 852$ nm one obtains $E_\mathrm{r} = 1.31 \times 10^{-11}$ eV. Thus, the typical depth of an optical lattice is 11 orders of magnitude lower than that of the lattices encountered in traditional solid-state physics. This implies that the characteristic frequencies of ultracold atoms in optical lattices fall into the lower kilohertz regime.

The pairs of counterpropagating beams needed to create optical lattices in one, two, or three dimensions can be realized either by splitting a laser beam in two, or by retro-reflecting a beam off a mirror. In the former case, a small frequency difference $\Delta\nu(t)$ introduced between the two split laser beams with the help of acousto-optic modulators makes the lattice move with velocity $v(t) = \Delta\nu(t)\lambda/2$ (Ben Dahanet al., 1996; Lignier et al., 2007; Madison et al., 1997; Madison et al., 1998; Niu et al., 1996; Sias et al., 2008). Therefore, in the laboratory frame of reference an atom then experiences the potential

$$V_\mathrm{lab}(x,t) = \frac{V_0}{2}\cos\left(2k_\mathrm{L}[x - X_0(t)]\right), \tag{22}$$

where

$$X_0(t) = \frac{\lambda}{2}\int_0^t \mathrm{d}\tau\, \Delta\nu(\tau). \tag{23}$$

When using retro-reflected beams, lattice motion can be achieved by mounting the mirror on a piezo-electric actuator, so that it shifts according to some prescribed protocol $X_0(t)$ (Alberti et al., 2009; Zenesini et al., 2009). As the shift range of such devices is in the micrometer regime, this method is suitable for inducing an oscillatory motion as needed for shaking lattices, but not for applying a constant acceleration.

In the following steps, the Schrödinger equation for the translational motion of an atom in the shifted lattice, governed by the Hamiltonian:

$$H_\mathrm{lab}(t) = \frac{p^2}{2M} + V_\mathrm{lab}(x,t) \tag{24}$$

is subjected to a unitary transformation to the frame of reference co-moving with the lattice. First, the corresponding shift in position is implemented by means of the unitary operator:

$$U_1 = \exp\left(\frac{\mathrm{i}}{\hbar}X_0(t)p\right), \tag{25}$$

implying

$$U_1 x U_1^\dagger = x + X_0(t) \tag{26}$$

and

$$U_1 \left(-\mathrm{i}\hbar\frac{\partial}{\partial t}\right) U_1^\dagger = -\mathrm{i}\hbar\frac{\partial}{\partial t} - \dot{X}_0(t)p, \tag{27}$$

thus leading to the new Hamiltonian

$$\widetilde{H}(t) = \frac{1}{2M}\left(p - M\dot{X}_0(t)\right)^2 + \frac{V_0}{2}\cos\left(2k_\mathrm{L}x\right) - \frac{M}{2}\dot{X}_0(t)^2. \tag{28}$$

Next, the shift of momentum in this expression is compensated through the unitary transformation

$$U_2 = \exp\left(-\frac{\mathrm{i}}{\hbar}M\dot{X}_0(t)x\right), \tag{29}$$

giving

$$U_2 p U_2^\dagger = p + M\dot{X}_0(t) \tag{30}$$

together with

$$U_2 \left(-\mathrm{i}\hbar\frac{\partial}{\partial t}\right) U_2^\dagger = -\mathrm{i}\hbar\frac{\partial}{\partial t} + M\ddot{X}_0(t)x. \tag{31}$$

Finally, the last term in Equation (28) can be transformed away using the operator

$$U_3 = \exp\left(-\frac{\mathrm{i}}{\hbar}\frac{M}{2}\int_0^t \mathrm{d}\tau\, \dot{X}_0^2(\tau)\right), \tag{32}$$

since

$$U_3 \left(-\mathrm{i}\hbar\frac{\partial}{\partial t}\right) U_3^\dagger = -\mathrm{i}\hbar\frac{\partial}{\partial t} + \frac{M}{2}\dot{X}_0^2(t). \tag{33}$$

The full transformation to the co-moving frame is then realized by the combined operation $U = U_3U_2U_1$, giving

$$U\left(H_\mathrm{lab}(t) - \mathrm{i}\hbar\partial_t\right)U^\dagger = H_0 + H_1(t) - \mathrm{i}\hbar\partial_t, \tag{34}$$

with

$$H_0 = \frac{p^2}{2M} + \frac{V_0}{2}\cos\left(2k_\mathrm{L}x\right) \tag{35}$$

denoting the single-particle Hamiltonian pertaining to the undriven lattice, and

$$H_1(t) = -F(t)x \tag{36}$$

introducing a homogeneous inertial force $F(t)$ acting in the co-moving frame, determined by the lattice motion according to

$$F(t) = -M\ddot{X}_0(t). \tag{37}$$

In particular, when a purely sinusoidal frequency shift with an initial phase ϕ is suddenly applied at $t = 0$,

$$\Delta\nu(t) = \begin{cases} 0, & t < 0, \\ \Delta\nu_{\max} \sin(\omega t + \phi), & t > 0, \end{cases} \tag{38}$$

Equations (22) and (23) give

$$V_{\text{lab}}(x,t) = \frac{V_0}{2} \cos\left(2k_{\text{L}}[x + L\{\cos(\omega t + \phi) - \cos(\phi)\}]\right) \tag{39}$$

for $t > 0$, so that the lattice is shaken in the laboratory frame with the amplitude

$$L = \frac{\lambda \Delta\nu_{\max}}{2\omega}. \tag{40}$$

According to Equation (23), one has $\dot{X}_0(t) = \lambda\Delta\nu(t)/2$. Therefore, this protocol (38) effectuates a sudden jump of the lattice's velocity at time $t = 0$, unless $\phi = 0$ or $\phi = \pi$. By virtue of Equation (37), the force felt by the atoms in the co-moving frame of reference then is composed of a monochromatic oscillating drive acting for $t > 0$, and of a delta-like kick acting at the moment of turn-on: Formally, one obtains

$$F(t) = -F_1 \cos(\omega t + \phi)\Theta(t) - \frac{F_1}{\omega} \sin(\phi)\delta(t), \tag{41}$$

where $\Theta(t)$ denotes the Heaviside function, and the driving amplitude is given by

$$F_1 = M\frac{\lambda}{2}\Delta\nu_{\max}\omega = ML\omega^2. \tag{42}$$

Needless to say, in reality the delta-kick experienced at $t = 0$ has a finite sharpness, determined by the short-time details of the actual velocity jump. Nonetheless, this kick has an important experimental consequence, as will be discussed later.

As a dimensionless measure of the shaking or driving strength we introduce the quantity

$$K_0 = \frac{F_1 d}{\hbar\omega} = \frac{\pi^2}{2}\frac{\omega}{\omega_{\text{r}}}\frac{L}{d}, \tag{43}$$

where $d = \lambda/2$ is the lattice constant. Thus, with driving frequencies on the order of the recoil frequency $\omega_{\text{r}} = E_{\text{r}}/\hbar$, and modulation amplitudes (40) on the order of the lattice constant, one can easily reach the nonperturbative regime $K_0 > 1$. It would be quite hard to realize corresponding conditions in laser-irradiated traditional solids without introducing, e.g., additional polarization effects, or even damaging the sample. Therefore, strongly shaken optical lattices may also be viewed as "strong-field simulators" which allow one to study even superstrong-field-induced multiphoton-like processes in periodic potentials, such as interband transitions, in their purest form (Arlinghaus & Holthaus, 2010).

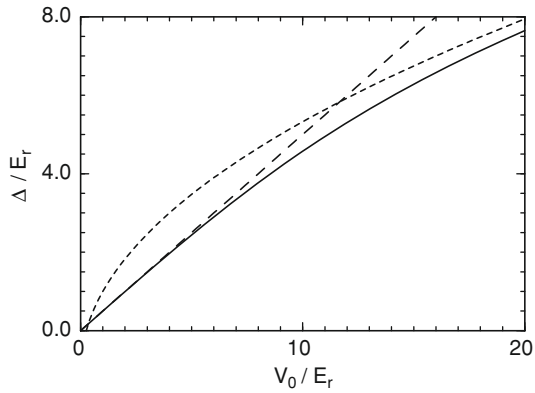

Figure 1 Exact energy gap Δ between the lowest two bands of an optical cosine lattice (20), measured in multiples of the recoil energy E_r (full line), in comparison with the shallow-lattice estimate (44) (long dashes), and with the deep-lattice estimate (45) (short dashes).

4. THE DRIVEN BOSE–HUBBARD MODEL

In principle, the time-periodic motion (39) always induces transitions between the unperturbed energy bands of the optical lattice. However, if the energy scale $\hbar\omega$ associated with the modulation frequency remains small compared to the energy gap Δ between the lowest two bands, and if the driving amplitude remains sufficiently low, the dynamics of driven ultracold atoms remain restricted to the lowest band at least to good approximation. Since the band structure of a cosine lattice (20) is determined by the characteristic values of the Mathieu equation (Slater, 1952), the known expansions of these values (Abramowitz & Stegun, 1965) can be employed for obtaining estimates of the gap width, resulting in

$$\Delta/E_r \approx V_0/(2E_r) \tag{44}$$

for shallow lattices, and

$$\Delta/E_r \approx 2\sqrt{V_0/E_r} - 1 \tag{45}$$

for fairly deep ones. Figure 1 constitutes proof that these two approximations indeed provide a reasonable estimate of the exact band gap for all V_0/E_r, if one switches from the shallow-lattice result (44) to the deep-lattice formula (45) at $V_0/E_r \approx 11.7$. As a reference point, the exact gap width is $\Delta = 4.572E_r$ for a lattice with depth $V_0 = 10E_r$.

In our experiments (Eckardt et al., 2009; Lignier et al., 2007; Sias et al., 2008; Zenesini et al., 2009) we work with Bose–Einstein condensates of ^{87}Rb consisting of about 5×10^4 atoms in a shaken 1D optical lattice ($\lambda = 852$ nm

or 842 nm) with depths V_0/E_r ranging from 3 to 10, employing scaled shaking frequencies $\hbar\omega/E_\mathrm{r}$ between roughly 0.1 and 2 (corresponding to $\omega/(2\pi)$ between 0.3 and 6 kHz). Under such conditions the single-band approximation is viable, provided the forcing is not too strong, since crossing the gap would require higher-order multiphoton-like transitions (Arlinghaus & Holthaus, 2010). In order to model these driven, interacting many-body systems we resort to the co-moving frame of reference, and then follow the standard route (Bloch et al., 2008; Jaksch et al., 1998; Jaksch & Zoller, 2005). Employing a basis of site-localized Wannier functions pertaining to the lowest Bloch band, and assuming a reasonable lattice depth $V_0/E_\mathrm{r} \gg 1$, it suffices to retain only the hopping matrix element J connecting neighboring sites. The accuracy of this approximation has been assessed quantitatively by Boers et al. (2007) and Eckardt et al. (2009); for instance, when $V_0/E_\mathrm{r} = 10$ the neglected matrix element connecting next-to-nearest neighbors is actually smaller than J by a factor of about 0.012. Moreover, the van der Waals length of alkali atoms typically amounts to just a few nanometers (Bloch et al., 2008) and thus is significantly smaller than the lattice constant $d = \lambda/2$, so that only the on-site interaction among the atoms has to be accounted for; this is done in terms of a parameter U which quantifies the interaction energy of one pair of atoms occupying the same lattice site (Schneider et al., 2009). In short, when adopting these three approximations (single-band, nearest-neighbor, and on-site), an ultracold gas of bosonic atoms in a time-periodically shaken optical lattice is described in the co-moving frame by the explicitly time-dependent many-body Hamiltonian[1] (Creffield & Monteiro, 2006; Eckardt et al., 2005b)

$$\widehat{H}(t) = \widehat{H}_0 + \widehat{H}_1(t), \tag{46}$$

where

$$\widehat{H}_0 = -J \sum_\ell \left(\hat{b}_\ell^\dagger \hat{b}_{\ell+1} + \hat{b}_{\ell+1}^\dagger \hat{b}_\ell \right) + \frac{U}{2} \sum_\ell \hat{n}_\ell (\hat{n}_\ell - 1) \tag{47}$$

is the standard Bose–Hubbard model for a 1D lattice (Fisher et al., 1989; Jaksch et al., 1998; Jaksch & Zoller, 2005), with $\hat{b}_\ell$ denoting the bosonic annihilation operator for atoms occupying the Wannier state at the ℓth site; $\hat{n}_\ell = \hat{b}_\ell^\dagger \hat{b}_\ell$ is the number operator for that site. Recalling that the position operator x mediating the inertial force built into the single-particle Hamiltonian (36) translates, on the many-body level, into $d \sum_\ell \ell \hat{n}_\ell$, with $d = \lambda/2$ for the distance between two sites, the time-periodic forcing is now introduced through

$$\widehat{H}_1(t) = K \cos(\omega t) \sum_\ell \ell \hat{n}_\ell, \tag{48}$$

[1] We use the "hat"-symbol to indicate operators acting on the bosonic Fock space.

where the strength K is related to the forcing amplitude (42) by $K = F_1 d$. Here we disregard an initial phase ϕ, which would refer to a sudden turn-on of the force, as in Equation (38). This driven 1D Bose–Hubbard model (46) may be extended to higher spatial dimensions (Zenesini et al., 2009); we remark that approximate expressions relating the parameters J and U to the lattice depth have been provided by Zwerger (2003) and Bloch et al. (2008).

5. INTERFERENCE PATTERNS PRODUCED BY FLOQUET STATES

It is essential to observe that the existence of Floquet states (1) hinges solely on the periodicity of the given Hamiltonian in time. Thus, besides the single-particle Floquet states which form the basis of the statistical considerations in Section 2, there also are Floquet states for periodically time-dependent, interacting many-body systems, such as periodically driven Bose gases, which incorporate both the periodic time-dependence and all interaction effects.

5.1 Signatures of Interacting Shaken Bose Gases

Here we are concerned, in particular, with the Floquet states of the driven Bose–Hubbard model (46), and their experimental signatures. In order to solve the quasienergy eigenvalue problem (10) for this model, the quasienergy operator $\widehat{H}(t) - \mathrm{i}\hbar\partial_t$ has to be diagonalized in the associated extended Hilbert space (Sambe, 1973), as reviewed in Section 2. To this end, let $\{n_\ell\}$ denote an admissible set of site-occupation numbers n_ℓ. The physical many-body Hilbert space then is spanned by the set of all Fock states

$$|\{n_\ell\}\rangle = \prod_\ell \frac{(\hat{b}_\ell^\dagger)^{n_\ell}}{\sqrt{n_\ell!}}|\mathrm{vac}\rangle, \tag{49}$$

where $|\mathrm{vac}\rangle$ is the "empty-lattice" state. A possible basis of the extended space would be provided by the products $|\{n_\ell\}\rangle \exp(\mathrm{i}m\omega t)$ with integer m. However, it is more useful here to employ the basis of Floquet–Fock states (or "dressed Fock states") given by

$$|\{n_\ell\}, m\rangle\rangle \equiv |\{n_\ell\}\rangle \exp\left\{-\mathrm{i}\frac{K}{\hbar\omega}\sin(\omega t)\sum_\ell \ell n_\ell + \mathrm{i}m\omega t\right\}, \tag{50}$$

which already diagonalize $\widehat{H}(t) - \mathrm{i}\hbar\partial_t$ for vanishing interwell hopping strength $J = 0$ (Eckardt & Holthaus, 2007; Eckardt et al., 2005b). Invoking the scalar product (11), in this basis the matrix of the quasienergy operator

has the structure

$$\langle\langle\{n'_\ell\}, m'|\widehat{H}(t) - \mathrm{i}\hbar\partial_t|\{n_\ell\}, m\rangle\rangle$$
$$= \delta_{m',m}\langle\{n'_\ell\}|\widehat{H}_{\mathrm{eff}} + m\hbar\omega|\{n_\ell\}\rangle + (1-\delta_{m',m})\langle\{n'_\ell\}|\widehat{V}|\{n_\ell\}\rangle, \qquad (51)$$

where $\widehat{H}_{\mathrm{eff}}$ is a time-independent Bose–Hubbard Hamiltonian of the familiar form (47), but with the hopping matrix element J multiplied by a zero-order Bessel function J_0 with the argument $K_0 = K/(\hbar\omega)$, resulting in the effective hopping strength

$$J_{\mathrm{eff}} = JJ_0\left(K/(\hbar\omega)\right). \qquad (52)$$

The operator $\widehat{V}$, which is off-diagonal with respect to the photon index m, contains nearest-neighbor couplings J scaled by higher-order Bessel functions $\pm J_{m-m'}\left(K/(\hbar\omega)\right)$ (Eckardt & Holthaus, 2007; Eckardt et al., 2005b). Thus, the diagonalization of the quasienergy matrix (51) constitutes a tremendous problem of a kind not usually considered in traditional many-body physics: Infinitely many $\widehat{H}_{\mathrm{eff}}$-blocks, each one corresponding to the full Hamiltonian matrix of a time-independent Bose–Hubbard model (47) with modified hopping matrix elements (52), are shifted against each other in energy by integer multiples of $\hbar\omega$, and are coupled by $\widehat{V}$-blocks. The latter blocks, in their turn, embody hopping elements which are multiplied by Bessel-function factors with indices reflecting the distance of the respective block from the main diagonal. In effect, these $\widehat{V}$-couplings cause multiphoton-like resonances among the states described by the shifted diagonal blocks (Eckardt & Holthaus, 2008b). While the physics of this problem has not yet been explored in full generality, its high-frequency regime is comparatively transparent. Namely, if $\hbar\omega$ is large compared to the two energy scales J and U (while remaining still small compared to the band gap Δ of the underlying optical lattice, so that the single-band treatment remains applicable), it is a good approximation to neglect the couplings induced by $\widehat{V}$ altogether, so that the driven system (46) reduces to an undriven system described by $\widehat{H}_{\mathrm{eff}}$, meaning that the effect of the time-periodic force essentially is to "renormalize" the hopping matrix element according to Equation (52). With the $\widehat{V}$-couplings removed, all $\widehat{H}_{\mathrm{eff}}$-blocks are equivalent, and returning from the extended to the physical Hilbert space is tantamount to considering only one such block from the outset. Since the ratio J/U governs the superfluid-to-Mott insulator transition intrinsic to the Bose–Hubbard model (Bloch et al., 2008; Fisher et al., 1989; Zwerger, 2003), the renormalization of J in response to high-frequency forcing implies that it is possible to induce that transition by adjusting the parameters of the driving force, while keeping the lattice depth and hence U constant (Eckardt & Holthaus, 2008a; Eckardt et al., 2005b). This type of coherent control over the superfluid-to-Mott insulator transition has

been demonstrated in a pioneering experiment by Zenesini et al. (2009). It involves adiabatic following of the $\widehat{H}_{\rm eff}$-ground state as the driving amplitude is slowly changed; this has meanwhile been studied in detail with the help of numerical simulations by Poletti and Kollath (2011).

As in the time-independent case, experimental information about the many-body state $|\psi(t)\rangle$ is obtained by time-of-flight absorption imaging: Switching off the time-periodically shaken lattice potential at some moment t, then letting the matter wave expand (neglecting interaction effects during that expansion), and finally recording its density in space after a sufficiently long expansion time yields the momentum distribution (Bloch et al., 2008; Zwerger, 2003)

$$\begin{aligned} n(p,t) &= \langle\psi(t)|\hat{a}^\dagger(p)\hat{a}(p)|\psi(t)\rangle \\ &= |\widetilde{w}(p)|^2 \sum_{r,s} \exp\left(\frac{\mathrm{i}}{\hbar}(r-s)pd\right) \langle\psi(t)|\hat{b}_r^\dagger \hat{b}_s|\psi(t)\rangle, \end{aligned} \tag{53}$$

where $\hat{a}(p)$ is the annihilation operator for a free-particle state with momentum p in the direction of the lattice, and $\widetilde{w}(p)$ is the Fourier transform of the Wannier function pertaining to the lowest Bloch band; again, $d = \lambda/2$ denotes the lattice constant. Thus, apart from the factor $|\widetilde{w}(p)|^2$ the observed momentum distribution is given by the Fourier transform of the system's one-particle density matrix $\langle\psi(t)|\hat{b}_r^\dagger \hat{b}_s|\psi(t)\rangle$. Let us now assume that for a given driving amplitude $K/(\hbar\omega)$, and hence for a given value of $J_{\rm eff}$, an eigenstate of $\widehat{H}_{\rm eff}$ with energy ε takes the form:

$$|\psi_{\rm eff}(t)\rangle = \exp(-\mathrm{i}\varepsilon t/\hbar) \sum_{\{n_\ell\}} \gamma_{\{n_\ell\}} |\{n_\ell\}\rangle \tag{54}$$

with certain coefficients $\gamma_{\{n_\ell\}}$. Under conditions such that the high-frequency approximation detailed above is valid, the corresponding many-body state in the driven optical lattice is then obtained by replacing the Fock states (49) in this expansion (54) by the Floquet–Fock states (50) with $m = 0$, say, resulting in

$$|\psi(t)\rangle = \exp(-\mathrm{i}\varepsilon t/\hbar) \sum_{\{n_\ell\}} \gamma_{\{n_\ell\}} |\{n_\ell\}\rangle \exp\left\{-\mathrm{i}\frac{K}{\hbar\omega}\sin(\omega t)\sum_\ell \ell n_\ell\right\}. \tag{55}$$

In order to evaluate the momentum distribution (53) for this particular many-body Floquet state (55) we then compute

$$\begin{aligned} \langle\psi(t)|\hat{b}_r^\dagger \hat{b}_s|\psi(t)\rangle = &\sum_{\{n_\ell\},\{n'_\ell\}} \gamma^*_{\{n'_\ell\}} \gamma_{\{n_\ell\}} \langle\{n'_\ell\}|\hat{b}_r^\dagger \hat{b}_s|\{n_\ell\}\rangle \\ &\times \exp\left\{-\mathrm{i}\frac{K}{\hbar\omega}\sin(\omega t)\sum_\ell \ell(n_\ell - n'_\ell)\right\}. \end{aligned} \tag{56}$$

The only nonvanishing matrix elements are those with $n_\ell = n'_\ell$ for $\ell \neq r, s$; together with $n'_r = n_r + 1$ and $n'_s = n_s - 1$. This implies

$$\sum_\ell \ell(n_\ell - n'_\ell) = -(r - s), \tag{57}$$

which allows us to take the phase factor appearing on the right-hand side of Equation (56) out of the sum, giving

$$\langle\psi(t)|\hat{b}_r^\dagger \hat{b}_s|\psi(t)\rangle = \langle\psi_{\text{eff}}|\hat{b}_r^\dagger \hat{b}_s|\psi_{\text{eff}}\rangle \exp\left\{\mathrm{i}(r-s)\frac{K}{\hbar\omega}\sin(\omega t)\right\}. \tag{58}$$

Inserting this result into the representation (53), we immediately obtain the momentum distribution provided by a single Floquet state of the driven Bose–Hubbard model (46) in the high-frequency regime:

$$n(p,t) = |\widetilde{w}(p)|^2 \sum_{r,s}\langle\psi_{\text{eff}}|\hat{b}_r^\dagger \hat{b}_s|\psi_{\text{eff}}\rangle \exp\left\{\frac{\mathrm{i}}{\hbar}(r-s)\left(pd + \frac{K}{\omega}\sin(\omega t)\right)\right\}, \tag{59}$$

where, by assumption, $|\psi_{\text{eff}}\rangle$ is the associated energy eigenstate of $\widehat{H}_{\text{eff}}$.

However, an important step is still missing in order to connect theory with experiment: The driven Bose–Hubbard model, with the inertial force being incorporated through the driving term (48), refers to the comoving frame of reference as considered in Section 3, whereas measurements usually are performed in the laboratory frame. Thus, in order to obtain the momentum distribution $n_{\text{lab}}(p_{\text{lab}}, t)$ as recorded by an observer in the laboratory frame, we still have to invert the transformation (30). This is done in the general case by writing

$$p = p_{\text{lab}} - M\dot{X}_0(t), \tag{60}$$

and through

$$p = p_{\text{lab}} - \frac{K}{\omega d}\sin(\omega t) \tag{61}$$

for the driven Bose–Hubbard model with forcing (48), as corresponding to a frequency variation $\Delta\nu(t) = \Delta\nu_{\max}\sin(\omega t)$ between the counterpropagating laser beams, or to lattice motion $\dot{X}_0(t) = L\omega\sin(\omega t)$, taking into account the relation (42) for the driving amplitude, together with the definition $K = F_1 d$. Therefore, we finally have

$$\begin{aligned} n_{\text{lab}}(p_{\text{lab}}, t) = {} & \left|\widetilde{w}\left(p_{\text{lab}} - K/(\omega d)\sin(\omega t)\right)\right|^2 \\ & \times \sum_{r,s}\exp\left(\frac{\mathrm{i}}{\hbar}(r-s)p_{\text{lab}}d\right)\langle\psi_{\text{eff}}|\hat{b}_r^\dagger \hat{b}_s|\psi_{\text{eff}}\rangle. \end{aligned} \tag{62}$$

This is quite a significant observation: The momentum distribution of a matter wave occupying a many-body Floquet state in a time-periodically shaken optical lattice (39) in the high-frequency regime equals that of the associated energy eigenstate of $\widehat{H}_{\text{eff}}$, obtained from the undriven Bose–Hubbard Hamiltonian (47) through the replacement of the hopping matrix element J by J_{eff} as defined in Equation (52), insofar as exactly the same Fourier transform of the one-particle density matrix appears in both cases. Hence, even though the position of the lattice is periodically shifted, the peak pattern observed in the laboratory frame does not move. The effect of the time-periodic shift is seen only in the *envelope* of that pattern, given by the Fourier transform $\widetilde{w}$ of the Wannier function, the argument of which is modulated periodically in time in accordance with Equation (61). Thus, apart from this modulation the experimental signature of the superfluid-to-Mott insulator transition occurring in shaken optical lattices upon changing the driving amplitude (Zenesini et al., 2009) is the same as that of the transition occurring in a stationary lattice in response to a variation of its depth (Bloch et al., 2008; Zwerger, 2003).

It may be useful to point out that the experimental signatures differ from the above description if the optical lattice is not shaken, but kept at rest, while the force is induced by means of the time-periodic modulation of a levitation gradient which "stirs" the condensate, as done in the experiments by Haller et al. (2010). In this latter situation the model (48) actually describes the driving force in the very reference frame in which the momentum distribution is recorded, so that one obtains an oscillating interference pattern given directly by Equation (59). In contrast, in the experiments reported by Lignier et al. (2007), Sias et al. (2008), Eckardt et al. (2009), and Zenesini et al. (2009); and in Section 6 below, the lattice is shaken in the laboratory frame according to Equation (39). Hence, here the "micromotion" is taken out of the interference pattern by means of Equation (61), which connects the momentum p in the co-moving frame to the momentum p_{lab} observed in the laboratory frame. The fact that the resulting interference pattern does not move in the laboratory frame (Eckardt & Holthaus, 2007, 2008a; Eckardt et al., 2005b) may sometimes facilitate its interpretation.

5.2 Signatures of Ideal Shaken Bose Gases

With respect to the Floquet condensates envisioned in Section 2, the case of an ideal Bose–Einstein condensate in a shaken optical lattice now is of particular interest. For vanishing interaction $U = 0$ the time-dependent Schrödinger equation for the model (46) can easily be solved exactly for any type of forcing described by a driving term

$$\widehat{H}_1(t) = -F(t)d\sum_{\ell} \ell \hat{n}_\ell, \tag{63}$$

without requiring a specific time-dependence of the force. Therefore, we abandon time-periodic forces and the Floquet picture for the time being, and consider an initial-value problem instead: We assume that $F(t)$ vanishes for $t < 0$, and is switched on sharply at $t = 0$, but is arbitrary otherwise. Generalizing the previous Equation (41), we thus impose a force

$$F(t) = -M\ddot{X}_0(t)\Theta(t) - M\dot{X}_0(0+)\delta(t), \tag{64}$$

where the second term accounts for the sudden velocity jump of the lattice from $\dot{X}_0(0-) = 0$ to an arbitrary value $\dot{X}_0(0+)$ at $t = 0$. Moreover, we consider a lattice with $M_L \gg 1$ sites and disregard finite-size effects, so that the operator

$$\hat{c}_k^\dagger(0) = \frac{1}{\sqrt{M_L}} \sum_\ell \exp(\mathrm{i}\ell k d)\hat{b}_\ell^\dagger \tag{65}$$

creates a particle in the Bloch state with quasimomentum $\hbar k$. We then assume that the initial state at $t = 0$ is an ideal N-particle condensate occupying such a Bloch state. Even if $k = 0$ might be the only experimentally realistic option here, we do not impose this restriction at this point. For $t > 0$, after the force has been turned on, the resulting N-particle wave function can then be written in the form:

$$|\psi_k(t)\rangle = \frac{1}{\sqrt{N!}}\left[\hat{c}_k^\dagger(t)\right]^N |\mathrm{vac}\rangle. \tag{66}$$

Here the creation operator $\hat{c}_k^\dagger(t)$, given by

$$\hat{c}_k^\dagger(t) = \exp\left(-\frac{\mathrm{i}}{\hbar}\int_0^t \mathrm{d}\tau\, E\left(q_k(\tau)\right)\right) \frac{1}{\sqrt{M_L}} \sum_\ell \exp\left(\mathrm{i}\ell q_k(t) d\right) \hat{b}_\ell^\dagger, \tag{67}$$

refers to a so-called Houston state, also known as an accelerated Bloch state (Eckardt et al., 2009; Houston, 1940). This nomenclature stems from the fact that the time-dependent wave number $q_k(t)$ appearing here has to obey the "semiclassical" acceleration law

$$\hbar\dot{q}_k(t) = F(t). \tag{68}$$

Therefore, using the particular connection (64) between the inertial force and the lattice motion, and requiring that $q_k(t)$ be equal to the wave number k of the initial state for $t < 0$, we have

$$\begin{aligned} q_k(t) &= k + \frac{1}{\hbar}\int_0^t \mathrm{d}\tau\, F(\tau) \\ &= k - \frac{M}{\hbar}\left(\dot{X}_0(t) - \dot{X}_0(0+)\right) - \frac{M}{\hbar}\dot{X}_0(0+) = k - \frac{M}{\hbar}\dot{X}_0(t) \end{aligned} \tag{69}$$

for $t > 0$, having properly accounted for the delta-kick at the moment of turn-on. Finally, the expression

$$E(k) = -2J \cos(kd) \tag{70}$$

appearing in the exponential of Equation (67) denotes the single-particle dispersion relation describing the energy band provided by the Hamiltonian (47) when $U = 0$.

For such a noninteracting N-particle wave function (66) the momentum distribution (53) is given, apart from the factor $|\widetilde{w}(p)|^2$, by

$$\sum_{r,s} \exp\left(\mathrm{i}(r-s)pd/\hbar\right) \langle \psi_k(t)|\hat{b}_r^\dagger \hat{b}_s|\psi_k(t)\rangle = N \sum_r \exp\left(\mathrm{i}r[p/\hbar - q_k(t)]d\right). \tag{71}$$

The return to the laboratory frame now is achieved with the help of Equation (60), and expression (69) for $q_k(t)$: Using these, one obtains

$$p/\hbar - q_k(t) = p_{\mathrm{lab}}/\hbar - k. \tag{72}$$

Therefore, the interference pattern provided by an ideal Houston condensate in time-of-flight absorption imaging again is stationary in the laboratory frame, and the peak positions are not affected by the force: Even after the force (64) has been switched on, the interference peaks are still permanently centered around the wave numbers $k \bmod (2\pi/d)$, as they had been for the unforced initial condensate. It needs to be stressed that this peculiar feature is crucially dependent on the delta-kick which accompanies the sudden turn-on of the force in the co-moving frame.

In particular, let us now consider a monochromatic oscillating force switched on instantaneously at $t = 0$ with starting phase ϕ according to Equation (41), which leads to

$$q_k(t) = k - \frac{F_1}{\hbar\omega} \sin(\omega t + \phi) \tag{73}$$

for $t > 0$. In this case there is a close relation between the N-particle Houston states (66), which have been constructed for $t > 0$ as solutions of an initial-value problem, and N-particle Floquet states, which presuppose a perfectly time-periodic force $F(t) = -F_1 \cos(\omega t + \phi)$ acting at *all* times t. In order to obtain these Floquet states, one only has to extend $q_k(t)$, as given by Equation (73), to all t, and use this expression in Equation (67), now to be considered for all t. Then the emerging "extended" Houston states (66) have the basic form (1): By construction, $q_k(t)$ is T-periodic, with $T = 2\pi/\omega$, but the energy integral in the exponent of Equation (67) is not. However,

writing

$$\exp\left(-\frac{\mathrm{i}}{\hbar}\int_0^t \mathrm{d}\tau\, E(q_k(\tau))\right) = \exp\left(-\frac{\mathrm{i}}{\hbar}\int_0^t \mathrm{d}\tau\, \left[E(q_k(\tau)) - \varepsilon(k)\right]\right)\exp\left(-\mathrm{i}\varepsilon(k)t/\hbar\right)$$

with the help of the one-cycle-averaged energies

$$\varepsilon(k) = \frac{1}{T}\int_0^T \mathrm{d}\tau\, E(q_k(\tau)) = -2JJ_0\left(\frac{F_1 d}{\hbar\omega}\right)\cos(kd), \tag{74}$$

the first of these exponentials is T-periodic and therefore part of the Floquet functions, whereas the occurrence of the averages (74) in the second exponential, accompanied by the time t, allows one to identify them as quasienergies. The Houston–Floquet states thus found are particularly simple examples of spatiotemporal Bloch waves, incorporating both the spatial periodicity of the lattice and the temporal periodicity of the driving force on equal footing. They are labeled by the same quantum numbers k as the customary, time-independent Bloch waves to which they reduce in the absence of the drive, while their time-evolution, apart from the time-periodic motion incorporated into the moving wave numbers $q_k(t)$, is specified by the quasienergies $\varepsilon(k)$ (Arlinghaus & Holthaus, 2011). Observing that one again encounters here the effective hopping matrix element J_{eff} introduced in Equation (52), the quasienergy-quasimomentum dispersion relation takes the form:

$$\varepsilon(k) = -2J_{\mathrm{eff}}\cos(kd) \mod \hbar\omega, \tag{75}$$

which differs from the original dispersion relation (70) of the undriven lattice only through the replacement of J by J_{eff}. That same replacement was seen before in the context of the interacting many-body system described by the driven Bose–Hubbard model (46), when constructing the approximate effective Hamiltonian $\widehat{H}_{\mathrm{eff}}$ pertaining to the high-frequency regime. In contrast, in the noninteracting case considered here no approximations have been made; Equation (75) holds exactly for all driving frequencies. The fact that the quasienergies (75) for the driven, noninteracting Bose–Hubbard model could be calculated by taking the time-averages (74) further suggests that these quasienergies do coincide with the corresponding mean energies (13), as considered in Section 2. Indeed, taking a single-particle Houston–Floquet state $|\psi_k(t)\rangle = |u_k(t)\rangle\exp\left(-\mathrm{i}\varepsilon(k)t/\hbar\right)$ as constructed above, one easily confirms the identity

$$\overline{E}(k) = \langle\langle u_k|\widehat{H}(t)|u_k\rangle\rangle = -2J_{\mathrm{eff}}\cos(kd), \tag{76}$$

so that here the mean energies of the Floquet states actually equal the quasienergies (75), disregarding their "mod $\hbar\omega$"-multiplicity. In the case of a general T-periodic single-particle Hamiltonian $H^{(1)}(t)$ with Floquet states (1) this is not the case, since then

$$\overline{E}_n = \langle\langle u_n|H^{(1)} - \mathrm{i}\hbar\partial_t|u_n\rangle\rangle + \langle\langle u_n|\mathrm{i}\hbar\partial_t|u_n\rangle\rangle = \varepsilon_n + \langle\langle u_n|\mathrm{i}\hbar\partial_t|u_n\rangle\rangle, \qquad (77)$$

as discussed in detail by Fainshtein et al. (1978).

Interestingly, the quasienergy band (75) "collapses" when $K_0 = F_1 d/(\hbar\omega)$ equals a zero of the J_0 Bessel function (Holthaus, 1992), implying that an arbitrary single-particle wave packet driven under such conditions cannot spread, but reproduces itself T-periodically. This phenomenon, termed "dynamic localization" (Dunlap & Kenkre, 1986), has recently been observed with dilute Bose–Einstein condensates in driven optical lattices (Arlinghaus et al., 2011; Eckardt et al., 2009; Lignier et al., 2007). With a view towards future applications, the dependence of the quasienergy band width on the driving strength also has been identified as a means of controlling transport in systems with attractive pairing interactions (Kudo et al., 2009).

Once again, it is instructive to compare the above results, obtained for a shaken optical lattice, to the corresponding physics when the lattice is at rest, while the condensate is stirred by a harmonically modulated levitation gradient (Haller et al., 2010). Then it is actually possible to impose an instantaneously turned-on oscillating force

$$\widetilde{F}(t) = -F_1 \cos(\omega t + \phi)\Theta(t) \qquad (78)$$

without the additional delta-kick present in Equation (41), which necessarily appears when an inertial force is abruptly turned on. The moving wave numbers $q_k(t)$, which previously had been determined in Equation (69) as solutions to the equation of motion (68), now have to be replaced by the solutions $\widetilde{q}(t)$ to the corresponding equation $\hbar\ddot{\widetilde{q}}(t) = \widetilde{F}(t)$, giving

$$\widetilde{q}(t) = k + \frac{1}{\hbar}\int_0^t \mathrm{d}\tau\, \widetilde{F}(\tau) = k + \frac{F_1}{\hbar\omega}\sin(\phi) - \frac{F_1}{\hbar\omega}\sin(\omega t + \phi) \qquad (79)$$

for $t > 0$, instead of Equation (73) above. Therefore, one formally has

$$\widetilde{q}(t) = q_{k+\Delta k}(t) \qquad (80)$$

with a wave-number shift

$$\Delta k = \frac{F_1}{\hbar\omega}\sin(\phi), \qquad (81)$$

which means that an additional momentum $\hbar\Delta k$ is imparted on the condensate particles when the stirring force is switched on rapidly, as described by

Equation (78). Thus, besides the micromotion the resulting time-of-flight absorption images would also show a shift of the peak positions. Both of these features are absent in experiments with shaken lattices: It really matters whether the condensate is "shaken" or "stirred"!

We note that Kudo and Monteiro (2011a, 2011b), focusing on stirring forces of the form (78), have suggested to introduce effective dispersion relations which also incorporate the initial phase ϕ. While one is free to adopt this viewpoint, it seems to obscure the conceptual simplicity of the Floquet approach: The quasienergy band (75) characterizes the time-periodically driven system as such, regardless of the way the drive has been switched on, that is, independent of the phase ϕ which parametrizes the sudden turn-on (78), or of any other parameters which specify other, equally possible turn-on protocols. Because this quasienergy band (75) actually consists of eigenvalues of the quasienergy operator it even provides a dispersion relation in the usual sense of solid-state physics which allows one to compute group velocities by taking its derivative, properly evaluated at that quantum number k around which the wave packet is centered (Arlinghaus & Holthaus, 2011).

With regard to shaken condensates, we may summarize our considerations as follows: If an ideal Bose–Einstein condensate in an optical lattice initially occupies a Bloch state with wave number k, and then is abruptly being shaken and thus subjected to the force (41) under single-band conditions, it permanently populates a single Floquet state labeled by the same wave number k, regardless of the phase ϕ.

6. EXPERIMENTAL RESULTS

In order to substantiate the relevance of the above ideal-gas considerations for laboratory experiments, we took time-of-flight absorption images of dilute ^{87}Rb-condensates released from shaken 1D optical lattices (39), employing various driving frequencies and amplitudes. In Figure 2 we display typical results obtained for a lattice with depth $V_0 = 9E_\mathrm{r}$, driven with frequency $\omega/2\pi = 1$ kHz and scaled amplitude $K/(\hbar\omega) = 1.85$. Under such conditions the single-band approximation is well justified; according to Equation (52), one has $J_\mathrm{eff} = 0.311J$. The drive was turned on quickly with a starting phase ϕ, as modeled by Equation (41), and the images were taken 10 driving cycles later. Hence, provided that the solution (66) to the initial-value problem for the ideal gas discussed in Section 5 describes the real laboratory system correctly, Equations (71) and (72) tell us that for *any* value of ϕ there should be stationary interference maxima at $p_\mathrm{lab} = 0 \bmod \hbar(2\pi/d)$, or

$$\frac{p_\mathrm{lab}}{p_\mathrm{r}} = 0 \bmod 2, \tag{82}$$

using the recoil momentum $p_r = \hbar k_L$ as reference scale. This expectation is fully confirmed in Figure 2. In all three cases considered there, with $\phi = 0, +\pi/2$, and $-\pi/2$, the central peak is located at $p_{lab} = 0$, as corresponding to a condensate occupying the Houston–Floquet state associated with the *minimum* of the quasienergy band (75). In addition there are side peaks at $p_{lab} = \pm 2p_r$, corresponding to the width $\hbar(2\pi/d) = 2p_r$ of the quasimomentum Brillouin zone. The left panel of Figure 2 depicts the time-resolved evolution of the positions of the respective interference maxima during a single cycle of the driving force. As anticipated, these positions remain practically constant in time, apart from apparent slight wiggles. The right panel of Figure 2 shows the modulation of the height of the side peaks during one driving cycle, which stems from the oscillating time-dependence of the argument p of the factor $|\tilde{w}(p)|^2$ determining the envelope of the interference pattern in accordance with Equation (62). For all values of the starting phase we observe practically the same signals, which is in line with the surmise that they are signatures of the same state.

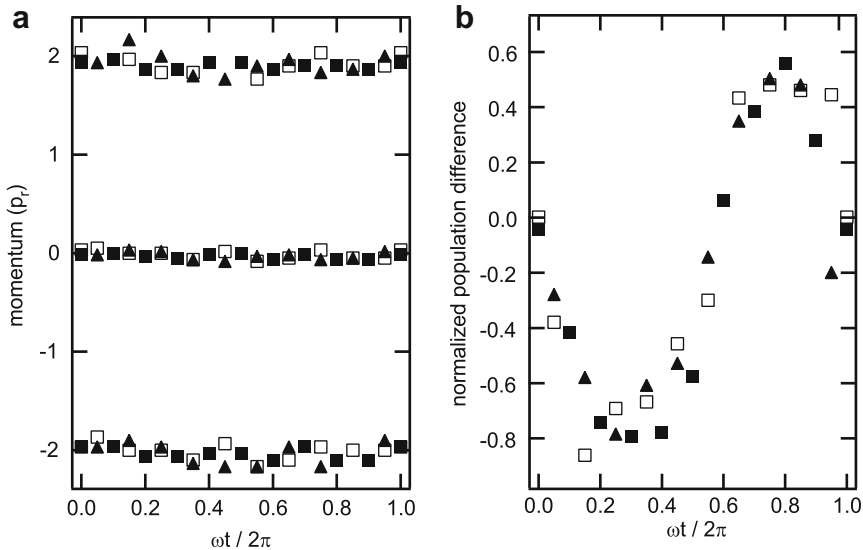

Figure 2 (a) Position of interference maxima observed in time-of-flight absorption imaging of condensates released from an optical lattice with depth $V_0 = 9E_r$, shaken with frequency $\omega/2\pi = 1$ kHz and scaled amplitude $K/(\hbar\omega) = 1.85$, during one shaking cycle. The starting phases ϕ of the drive are 0 (solid squares), $+\pi/2$ (open squares), and $-\pi/2$ (solid triangles); the images were taken 10 driving cycles after its turn-on. The maxima are centered around positions corresponding to momenta $p_{lab} = 0, \pm 2p_r$. (b) Modulation of the population difference of the side peaks during one shaking cycle. All three starting phases [symbols as in (a)] give rise to the same curve.

Therefore, we interpret the data displayed in Figure 2 as experimental signatures of Floquet condensates: The existence of a stationary, stable and lasting interference pattern indicates that the driven Bose gas actually tends to occupy a single Houston–Floquet state. The fact that this pattern is centered around $p_{\mathrm{lab}} = 0 \bmod 2\,p_{\mathrm{r}}$ implies that this state is the one at the bottom of the quasienergy band (75), which, by virtue of Equation (76), also is the one equipped with the lowest mean energy (13). This is not surprising, because we are starting with a condensate occupying the Bloch state $k = 0$, and because a drive of the form (41) does not change the quantum number k when it is turned on.

If a Floquet condensate is to be regarded as an entity of its own, then it should behave as such when probed by a weak force acting on top of the time-periodic, driving one. This is actually the case, as illustrated by a sequence of further measurements summarized in Figure 3: Here we consider a lattice with depth $V_0 = 10E_{\mathrm{r}}$ driven by an oscillating force with an additional weak static component, written as

$$F(t) = \big(-F_0 - F_1 \cos(\omega t)\big)\,\Theta(t), \tag{83}$$

so that the time-dependent wave numbers (69) now become

$$q_k(t) = k - \frac{F_0 t}{\hbar} - \frac{F_1}{\hbar\omega}\sin(\omega t) \tag{84}$$

for $t > 0$, disregarding an initial phase ϕ from the outset. Therefore, the system undergoes a pure Bloch oscillation when $F_1 = 0$: In response to a static force of strength F_0, one wave-number Brillouin zone of width $2\pi/d$ is then traversed at uniform "speed" $F_0/\hbar$ within the Bloch time

$$T_{\mathrm{B}} = \frac{2\pi\hbar}{F_0 d}, \tag{85}$$

and the periodicity of the energy-quasimomentum relation (70) in k gives rise to an oscillating wave-packet motion, as long as interband transitions remain negligible (Zener, 1934). We fix the Bloch frequency $\omega_{\mathrm{B}}/2\pi = 1/T_{\mathrm{B}}$ at 242.4 Hz, and the driving frequency $\omega/2\pi$ at 3.0 kHz, more than 12 times higher. This clear separation of time scales implies transparent dynamics: Essentially, the oscillating component of the force (83) "dresses" the gas, making it condense into the Floquet state associated with the minimum of the quasienergy–quasimomentum relation (75), as before. The relatively weak static component then merely probes this dressed system, making it behave as an undressed condensate would if Equation (75) actually were the *energy* dispersion relation (Arlinghaus & Holthaus, 2011).

The signatures of such dynamics are again visible in time-of-flight absorption images. We expect stationary interference peaks, corresponding to the minima of the dispersion relation (75), while the argument

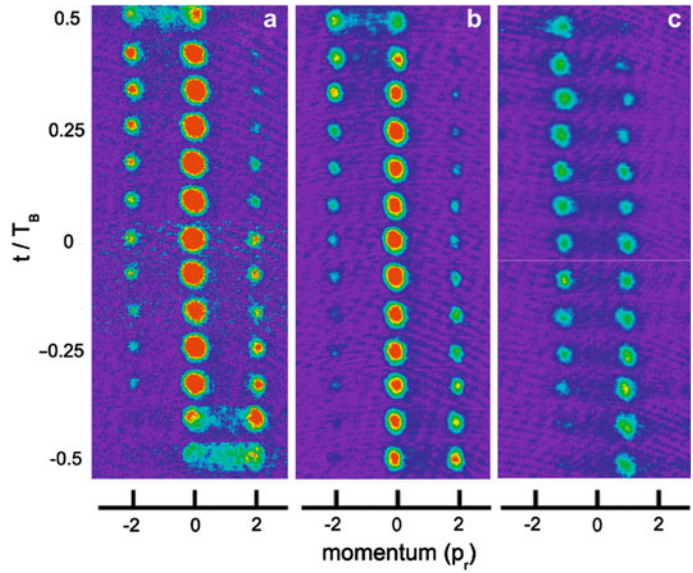

Figure 3 (Color online) Bloch oscillations in driven optical lattices ($V_0/E_r = 10$), recognizable as shifts of the interference pattern in time by one Brillouin zone of width $2p_r$ within one Bloch cycle T_B. The Bloch frequency is set to $\omega_B/2\pi = 242.4$ Hz, whereas the driving frequency is $\omega/2\pi = 3$ kHz. The dimensionless driving amplitudes $K/(\hbar\omega)$ correspond to 0, 1.5, and 4 (left to right). In (a), and to a lesser extent in (b), the pattern appears slightly smeared at times $t/T_B = \pm 1/2$, due to the occurrence of a dynamical instability. Note that the peak positions in (c) are centered around the edges $\pm p_r = \pm\hbar\pi/d$ of the quasimomentum Brillouin zone.

of the envelope-giving function $|\widetilde{w}(p)|^2$ in Equation (62) evolves in time as

$$\frac{p}{p_r} = \frac{p_{lab}}{p_r} - 2\frac{t}{T_B} - \frac{K/(\hbar\omega)}{\pi}\sin(\omega t), \tag{86}$$

with $K = F_1 d$. This is precisely what is seen in Figure 3: Here we show absorption images obtained from condensates released at times $t_i/T_B = i/12$ with $i = -6, -5, \ldots, 5, 6$, spanning one full Bloch cycle T_B (negative times here formally correspond to negative forces F_0 in Equation (83)). In the leftmost panel we consider $K/(\hbar\omega) = 0$, so that we are dealing with the bare system undergoing an undisturbed Bloch oscillation (Morsch et al., 2001), corresponding to an apparent displacement of the entire pattern by one Brillouin zone after one Bloch cycle. At $t/T_B = \pm 1/2$, when $q_k(t) = \pm\pi/d$ and the system passes the zone boundaries, a familiar dynamical instability occurs (Zheng et al., 2004), which becomes visible as a slight blurring of the peaks.

The middle panel shows the corresponding pictures obtained for $K/(\hbar\omega) = 1.5$, so that $J_{\mathrm{eff}} = 0.512\,J$: Indeed this set of images looks quite similar to the previous one, validating our view of a "dressed condensate" emerging through the application of the strong oscillating component of the force (83), and then responding to the static component like a bare one with a renormalized hopping matrix element J_{eff}. The effective reduction of J by a factor of about one half also leads to a notable reduction of the dynamical instability (Zheng et al., 2004).

The third panel finally shows the images obtained for $K/(\hbar\omega) = 4$, resulting in a *negative* effective hopping element, $J_{\mathrm{eff}} = -0.397\,J$. This means that the minima of the quasienergy dispersion (75) are now centered at the zone boundaries $k = \pm\,\pi/d$, where the maxima of the original dispersion (70) had been. Somewhat surprisingly, the gas spontaneously condenses into the associated Floquet state, leaving its signature in the form of two interference maxima neatly centered around $p = \pm p_{\mathrm{r}}$. This strongly dressed system then again performs a Bloch oscillation, as witnessed by the already familiar apparent displacement of the entire pattern by one quasimomentum Brillouin zone per Bloch cycle.

Thus, our system actively seems to select the corresponding Floquet state with the lowest mean energy, and seems to condense "by itself" into that state, as has also been reported by Lignier et al. (2007) for the case of purely sinusoidal driving. This finding goes beyond the ideal-gas picture, and requires further studies. It is underlined by a related observation: If we instantaneously change the driving amplitude such that the absolute magnitude of J_{eff} is preserved, but its sign is reversed, the original interference pattern caused by the initial state gradually vanishes, and the new pattern signaling the target state at the opposite band edge establishes itself within a few driving cycles. This process occurs in either direction, and appears to be fully reversible. This finding also implies that the dressed condensates settling down at the boundaries of the Brillouin zone when J_{eff} is negative actually are *stable*.

Such experiments involving a sudden change of J_{eff} are reminiscent of "quenching" experiments in which a parameter of a time-independent trapping potential is varied instantaneously, and the ensuing relaxation dynamics are observed (Dziarmaga, 2010; Polkovnikov et al., 2011). However, it is uncertain at this point whether our observations fit into this picture, and the underlying relaxation mechanism—if it really is one—needs to be understood in detail, keeping in mind the fact that the system is isolated and thus cannot get rid of excess energy. Still, in view of the preliminary thoughts put forward in Section 2, an interesting possibility suggests itself: The equilibrium state approached by a time-periodically driven, isolated Bose gas is determined not by usual thermodynamics, but by "periodic thermodynamics" in the sense of Kohn (2001), possibly

involving a generalized temperature Θ which depends on—and can, therefore, be controlled by—the external drive.

7. CONCLUSIONS

In a nutshell, the main results of the present study are encoded in Figure 3: The observation that the middle panel of this figure closely resembles the leftmost one indicates that there are Floquet condensates, that is, macroscopically occupied Floquet states of time-periodically forced Bose gases; the observation that the interference maxima are centered at the Brillouin zone edges when the effective hopping matrix element is negative, as seen in the rightmost panel, indicates that the Floquet condensate is carried by the Floquet state with the lowest mean energy. It remains to be seen whether these conclusions, drawn from one particular laboratory setting, also hold under more general circumstances.

The observation of stable interference patterns in the presence of the time-periodic forcing gives strong support to the surmise, formulated in Section 2, that time-periodically driven, weakly interacting Bose gases confined by trapping potentials which forbid their escape effectively constitute *equilibrium* systems, rather than nonequilibrium ones; the equilibrium state being characterized by a constant distribution of Floquet-state occupation numbers. Under conditions such that the mean-energy constraint (14) is valid, the expected distribution is the Bose–Einstein distribution (17), with the mean energies of the single-particle Floquet states replacing the single-particle energies appearing in time-independent situations. That distribution is characterized by two parameters α and γ, corresponding to the generalized chemical potential ν and to the generalized temperature Θ introduced in Equations (18) and (19). If this suggestion could be confirmed, it would open up further avenues of research: Also including fermions, a time-periodically driven, isolated quantum gas should establish a temperature of its own, so that it might be interesting to explore, e.g., whether an already ultracold gas can be made even colder by applying an external time-periodic force. In any case, these tentative speculations clearly indicate that time-periodically driven quantum gases offer much more than mere visualizations of already known condensed-matter phenomena; in fact, they require the development of new concepts for time-dependent quantum many-body dynamics.

ACKNOWLEDGEMENTS

M.H. acknowledges support from the Deutsche Forschungsgemeinschaft under Grant No. HO 1771/6. He also thanks E. Haller for a discussion

concerning experiments performed with non-shaken optical lattices (Haller et al., 2010). E.A., D.C., and O.M. acknowledge support from the E.U. through Grant No. 225187-NAMEQUAM, and from MIUR through PRIN2009. They also thank C. Sias, H. Lignier, and A. Zenesini for their assistance.

REFERENCES

Albramowitz, M., & Stegun, I. A. (Eds.), (1965). *Handbook of mathematical functions*. New York: Dover, pp.

Alberti, A., Ivanov, V. V., Tino, G. M., & Ferrari, G. (2009). Engineering the quantum transport of atomic wavefunctions over macroscopic distances. *Nature Physics, 5*, 547–550.

Arlinghaus, S., & Holthaus, M. (2010). Driven optical lattices as strong-field simulators. *Physical Review A, 81*, 063612.(4 pages)

Arlinghaus, S., & Holthaus, M. (2011). Generalized acceleration theorem for spatiotemporal Bloch waves. *Physical Review B, 84*, 054301.(11 pages)

Arlinghaus, S., Langemeyer, M., & Holthaus, M. (2011). Dynamic localization in optical lattices. In S. Keshavamurthy, & P. Schlagheck (Eds.), *Dynamical tunneling – Theory and experiment* (pp. 289–310). Boca Raton, FL: Taylor and Francis/CRC Press.

Ben Dahan, M., Peik, E., Reichel, J., Castin, Y., & Salomon, C. (1996). Bloch oscillations of atoms in an optical potential. *Physical Review Letters, 76*, 4508–4511.

Bloch, I., Dalibard, J., & Zwerger, W. (2008). Many-body physics with ultracold gases. *Reviews of Modern Physics, 80*, 885–964.

Boers, D. J., Goedeke, B., Hinrichs, D., & Holthaus, M. (2007). Mobility edges in bichromatic optical lattices. *Physical Review A, 75*, 063404.(6 pages)

Breuer, H. P., & Holthaus, M. (1991). A semiclassical theory of quasienergies and Floquet wave functions. *Annals of Physics, 211*, 249–291.

Breuer, H. P., Huber, W., & Petruccione, F. (2000). Quasistationary distributions of dissipative nonlinear quantum oscillators in strong periodic driving fields. *Physical Review E, 61*, 4883–4889.

Bunimovich, L., Jauslin, H. R., Lebowitz, J. L., Pellegrinotti, A., & Nielaba, P. (1991). Diffusive energy growth in classical and quantum driven oscillators. *Journal of Statistical Physics, 62*, 793–817.

Chen, Y. -A., Nascimbène, S., Aidelsburger, M., Atala, M., Trotzky, S., Bloch, I. (2011). Controlling correlated tunneling and superexchange interactions with AC-driven optical lattices. *Physical Review Letters, 107*, 210405.(4 pages)

Chu, S. -I., & Telnov, D. A. (2004). Beyond the Floquet theorem: Generalized Floquet formalisms and quasienergy methods for atomic and molecular multiphoton processes in intense laser fields. *Physics Reports, 390*, 1–131.

Creffield, C. E., & Monteiro, T. S. (2006). Tuning the Mott transition in a Bose–Einstein condensate by multiple photon absorption. *Physical Review Letters, 96*, 210403.(4 pages)

Drese, K., & Holthaus, M. (1997). Exploring a metal–insulator transition with ultracold atoms in standing light waves?. *Physical Review Letters, 78*, 2932–2935.

Dunlap, D. H., & Kenkre, V. M. (1986). Dynamic localization of a charged particle moving under the influence of an electric field. *Physical Review B, 34*, 3625–3633.

Dziarmaga, J. (2010). Dynamics of a quantum phase transition and relaxation to a steady state. *Advances in Physics, 59*, 1063–1189.

Eckardt, A., Hauke, P., Soltan-Panahi, P., Becker, C., Sengstock, K., Lewenstein, M. (2010). Frustrated quantum antiferromagnetism with ultracold bosons in optical lattices. *Europhysics Letters, 89*, 10010.(6 pages)

Eckardt, A., & Holthaus, M. (2007). AC-induced superfluidity. *Europhysics Letters, 80*, 50004. (6 pages)

Eckardt, A., & Holthaus, M. (2008a). Dressed matter waves. *Journal of Physics: Conference Series, 99*, 012007.(14 pages). Available from http://www.iop.org/EJ/toc/1742-6596/99/1

Eckardt, A., & Holthaus, M. (2008b). Avoided-level-crossing spectroscopy with dressed matter waves. *Physical Review Letters, 101*, 245302.(4 pages)
Eckardt, A., Holthaus, M., Lignier, H., Zenesini, A., Ciampini, D., Morsch, O., et al. (2009). Exploring dynamic localization with a Bose–Einstein condensate. *Physical Review A, 79*, 013611.(7 pages)
Eckardt, A., Jinasundera, T., Weiss, C., & Holthaus, M. (2005). Analog of photon-assisted tunneling in a Bose–Einstein condensate. *Physical Review Letters, 95*, 200401.(4 pages)
Eckardt, A., Weiss, C., & Holthaus, M. (2005). Superfluid–insulator transition in a periodically driven optical lattice. *Physical Review Letters, 95*, 260404.(4 pages)
Einstein, A. (1924). Quantentheorie des einatomigen idealen Gases. *Sitzungsberichte der Preussischen Akademie der Wissenschaften, XXII* (pp. 261–267). Gesamtsitzung.
Einstein, A. (1925). Quantentheorie des einatomigen idealen Gases. Zweite Abhandlung. *Sitzungsberichte der Preussischen Akademie der Wissenschaften, I*. Sitzung der physikalisch-mathematischen Klasse (pp. 3–14).
Fainshtein, A. G., Manakov, N. L., & Rapoport, L. P. (1978). Some general properties of quasi-energetic spectra of quantum systems in classical monochromatic fields. *Journal of Physics B – Atomic Molecular and Optical Physics, 11*, 2561–2577.
Fisher, M. P. A., Weichman, P. B., Grinstein, G., & Fisher, D. S. (1989). Boson localization and the superfluid–insulator transition. *Physical Review B, 40*, 546–570.
Floquet, G. (1883). Sur les équations différentielles linéaires à coefficients périodiques. *Annales scientifiques de l'École Normale Supérieure, 12*, 47–88.
Haller, E., Hart, R., Mark, M. J., Danzl, J. G., Reichsöllner, L., Nägerl, H. -C. (2010). Inducing transport in a dissipation-free lattice with super Bloch oscillations. *Physical Review Letters, 104*, 200403.(4 pages)
Holthaus, M. (1992). Collapse of minibands in far-infrared irradiated superlattices. *Physical Review Letters, 69*, 351–354.
Houston, W. V. (1940). Acceleration of electrons in a crystal lattice. *Physical Review, 57*, 184–186.
Howland, J.S. (1992a). Quantum stability. In *Schrödinger operators: The quantum mechanical manybody problem. Lecture notes in physics* Vol. 403 Springer-Verlag. New York:, pp. 100–122.
Howland, J. S. (1992b). Stability of quantum oscillators. *Journal of Physics A – Mathematical and General, 25*, 5177–5181.
Ivanov, V. V., Alberti, A., Schioppo, M., Ferrari, G., Artoni, M., Chiofalo, M. L., et al. (2008). Coherent delocalization of atomic wave packets in driven lattice potentials. *Physical Review Letters, 100*, 043602.(4 pages)
Jaksch, D., Bruder, C., Cirac, J. I., Gardiner, C. W., & Zoller, P. (1998). Cold bosonic atoms in optical lattices. *Physical Review Letters, 81*, 3108–3111.
Jaksch, D., & Zoller, P. (2005). The cold atom Hubbard toolbox. *Annals of Physics, 315*, 52–79.
Ketzmerick, R., & Wustmann, W. (2010). Statistical mechanics of Floquet systems with regular and chaotic states. *Physical Review E, 82*, 021114.(16 pages)
Kierig, E., Schnorrberger, U., Schietinger, A., Tomkovic, J., & Oberthaler, M. K. (2008). Single-particle tunneling in strongly driven double-well potentials. *Physical Review Letters, 100*, 190405.(4 pages)
Kohn, W. (2001). Periodic thermodynamics. *Journal of Statistical Physics, 103*, 417–423.
Kuchment, P. (1993). *Floquet theory for partial differential equations*. Basel: Birkhäuser.
Kudo, K., Boness, T., & Monteiro, T. S. (2009). Control of bound-pair transport by periodic driving. *Physical Review A, 80*, 063409.(6 pages)
Kudo, K., & Monteiro, T. S. (2011). Theoretical analysis of super-Bloch oscillations. *Physical Review A, 83*, 053627.(6 pages)
Kudo, K., & Monteiro, T. S. (2011b). Periodically-driven cold atoms: The role of the phase (10 pages). Available from: <arXiv:1008.2096v8>.
Lignier, H., Sias, C., Ciampini, D., Singh, Y., Zenesini, A., Morsch, O., et al. (2007). Dynamical control of matter-wave tunneling in periodic potentials. *Physical Review Letters, 99*, 220403. (4 pages)
London, F. (1938). On the Bose–Einstein condensation. *Physical Review, 54*, 947–954.
Madison, K. W., Bharucha, C. F., Morrow, P. R., Wilkinson, S. R., Niu, Q., Sundaram, B., et al. (1997). Quantum transport of ultracold atoms in an accelerating optical potential. *Applied Physics B, 65*, 693–700.

Madison, K. W., Fischer, M. C., Diener, R. B., Niu, Q., & Raizen, M. G. (1998). Dynamical Bloch band suppression in an optical lattice. *Physical Review Letters, 81*, 5093–5096.

Ma, R., Tai, M. E., Preiss, P. M., Bakr, W. S., Simon, J., Greiner, M. (2011). Photon-assisted tunneling in a biased strongly correlated Bose gas. *Physical Review Letters, 107*, 095301.(4 pages)

Morsch, O., Müller, J. H., Cristiani, M., Ciampini, D., & Arimondo, E. (2001). Bloch oscillations and mean-field effects of Bose–Einstein condensates in 1D optical lattices. *Physical Review Letters, 87*, 140402.(4 pages)

Morsch, O., & Oberthaler, M. (2006). Dynamics of Bose–Einstein condensates in optical lattices. *Reviews of Modern Physics, 78*, 179–215.

Niu, Q., Zhao, X. -G., Georgakis, G. A., & Raizen, M. G. (1996). Atomic Landau–Zener tunneling and Wannier–Stark ladders in optical potentials. *Physical Review Letters, 76*, 4504–4507.

Pathria, R. K. (1996). *Statistical mechanics* (2nd ed.). Oxford: Butterworth-Heinemann.

Peik, E., Ben Dahan, M., Bouchoule, I., Castin, Y., & Salomon, C. (1997). Bloch oscillations of atoms, adiabatic rapid passage, and monokinetic atomic beams. *Physical Review A, 55*(4), 2989–3001.

Poletti, D., & Kollath, C. (2011). Slow quench dynamics of periodically driven quantum gases. *Physical Review A, 84*, 013615.(9 pages)

Polkovnikov, A., Sengupta, K., Silva, A., & Vengalattore, M. (2011). Nonequilibrium dynamics of closed interacting quantum systems. *Reviews of Modern Physics, 83*, 863–883.

Ritus, V. I. (1967). Shift and splitting of atomic energy levels by the field of an electromagnetic wave. *Soviet Physics – Journal of Experimental and Theoretical Physics, 24*, 1041–1044. (Originally published 1966 in Zh. Eksp. Teor. Fiz. 51, 1544–1549)

Sambe, H. (1973). Steady states and quasienergies of a quantum-mechanical system in an oscillating field. *Physical Review A, 7*, 2203–2213.

Schneider, P. -I., Grishkevich, S., & Saenz, A. (2009). Ab initio determination of Bose–Hubbard parameters for two ultracold atoms in an optical lattice using a three-well potential. *Physical Review A, 80*, 013404.(13 pages)

Shirley, J. H. (1965). Solution of the Schrödinger equation with a Hamiltonian periodic in time. *Physical Review, 138*, B979–B987.

Sias, C., Lignier, H., Singh, Y. P., Zenesini, A., Ciampini, D., Morsch, O., et al. (2008). Observation of photon-assisted tunneling in optical lattices. *Physical Review Letters, 100*, 040404. (4 pages)

Slater, J. C. (1952). A soluble problem in energy bands. *Physical Review, 87*, 807–835.

Struck, J., Ölschläger, C., Le Targat, R., Soltan-Panahi, P., Eckardt, A., Lewenstein, M., et al. (2011). Quantum simulation of frustrated classical magnetism in triangular optical lattices. *Science, 333*, 996–999.

Tokuno, A., & Giamarchi, T. (2011). Spectroscopy for cold atom gases in periodically phase-modulated optical lattices. *Physical Review Letters, 106*, 205301.(4 pages)

Tsuji, N., Oka, T., Werner, P., & Aoki, H. (2011). Dynamical band flipping in fermionic lattice systems: An ac-field-driven change of the interaction from repulsive to attractive. *Physical Review Letters, 106*, 236401.(4 pages)

Zel'dovich, Ya. B. (1967). The quasienergy of a quantum-mechanical system subjected to a periodic action. *Soviet Physics – Journal of Experimental and Theoretical Physics, 24*, 1006–1008. (Originally published 1966 in Zh. Eksp. Teor. Fiz. 51, 1492–1495)

Zener, C. (1934). A theory of the electrical breakdown of solid dielectrics. *Proceedings of the Royal Society of London Series A, 145*, 523–529.

Zenesini, A., Lignier, H., Ciampini, D., Morsch, O., & Arimondo, E. (2009). Coherent control of dressed matter waves. *Physical Review Letters, 102*, 100403.(4 pages)

Zheng, Y., Koštrun, M., & Javanainen, J. (2004). Low-acceleration instability of a Bose–Einstein condensate in an optical lattice. *Physical Review Letters, 93*, 230401.(4 pages)

Zwerger, W. (2003). Mott–Hubbard transition of cold atoms in optical lattices. *Journal of Optics B – Quantum and Semiclassical Optics, 5*, S9–S16.